PROCEEDINGS B

royalsocietypublishing.org/rspb

Research

Cite this article: Scherer CR, Steell E, Upchurch P. 2026 Drivers and mechanisms of convergent forelimb reduction in non-avian theropod dinosaurs. *Proc. R. Soc. B* **293**: 20260528.
https://doi.org/10.1098/rspb.2026.0528

Received: 2 March 2026
Accepted: 10 April 2026

Subject Category:
Palaeobiology

Subject Areas:
ecology, evolution, palaeontology

Keywords:
cranial robusticity, gigantism, convergent evolution, Theropoda, forelimb reduction

Author for correspondence:
Charlie Roger Scherer
e-mail: cscherer2002@gmail.com

Drivers and mechanisms of convergent forelimb reduction in non-avian theropod dinosaurs

Charlie Roger Scherer[1], Elizabeth Steell[2,3] and Paul Upchurch[1]

[1]Department of Earth Sciences, University College London, London WC1E 6BT, UK
[2]Department of Earth Sciences, University of Cambridge, Cambridge CB3 0EQ, UK
[3]Girton College, University of Cambridge, Cambridge CB3 0JG, UK

CRS, 0009-0005-5846-9789; ES, 0000-0002-3999-3500; PU, 0000-0002-8823-4164

Forelimb reduction has been observed in numerous and disparate non-avian theropod dinosaurs, resulting in the hypothesis that reduced forelimbs evolved convergently. Clades with reduced forelimbs also possess high degrees of cranial robusticity and gigantic body sizes. Here, we provide a novel quantification of forelimb reduction across Theropoda, and create and implement a cranial robusticity scoring system, and analyse this dataset using bivariate and comparative phylogenetic analyses. Results indicate that forelimb reduction is strongly correlated with cranial robusticity and gigantism. Reduced/vestigial forelimbs evolved in at least five theropod lineages in concert with increased cranial robusticity and gigantism. Abelisaurids, carcharodontosaurids and tyrannosaurids show the greatest forelimb reduction relative to the skull. Repeated forelimb reduction across theropods was facilitated by increased cranial robusticity and greater body size that was potentially influenced by an upward trend in prey body size. These events resulted in a shift from subduing prey using grasping forelimbs to using powerful bites and robust skulls.

1. Introduction

Theropod dinosaurs constitute one of the most successful radiations of terrestrial vertebrates, with a fossil record extending back to the Late Triassic [1]. Among Mesozoic dinosaurs, non-avian theropods underwent major taxic, ecological and morphological diversification throughout the Jurassic and Cretaceous until their extinction at the close of the Cretaceous [2–4]. During this period, non-avian theropods achieved a cosmopolitan distribution [5] and occupied a broad range of ecological niches across terrestrial, arboreal, littoral and possibly aquatic habitats [6–10]. Body size disparity across theropod diversity is also particularly high [11] with multiple clades having evolved gigantism [12].

Non-avian theropod diversity is remarkable, and more than two centuries of study of these dinosaurs has resulted in the recognition of myriad theropod lineages, many of which were mutually contemporaneous during the Mesozoic [13]. Much of non-avian theropod morphological variation is apparent in the skull and forelimbs, with the robusticity and proportional size of the forelimb and skull varying across theropod phylogeny. In recent years, distinct trends of forelimb reduction and/or vestigialization have been observed in at least four distantly related non-avian, carnivorous theropod lineages: Abelisauridae, Alvarezsauria, Carcharodontosauridae and Tyrannosauridae [14–17]. Despite the absolute reduction in the forelimbs of these clades having been known for decades [18,19], the convergent evolution of this trait has only recently been rigorously analysed [17,20].

THE ROYAL SOCIETY PUBLISHING

Among the clades in which forelimb reduction (particularly element shortening) has been observed, trends of increasing gigantism (≥ 1000 kg body mass), super-gigantism (≥ 2500 kg body mass) and cranial ornamentation and robusticity have also been observed [12]. This suggests that forelimb reduction may be causally associated with increases in body size and increasing cranial robusticity. This phenomenon could be interpreted as being merely an allometric by-product of growth [21]. However, Canale *et al.* [17] showed that the convergent evolution of reduced forelimbs in gigantic theropods is not attributable to a single shared underlying pattern of allometric growth. For example, the carcharodontosaurids *Acrocanthosaurus* and *Meraxes* are similar in body size but display dissimilar forelimb reduction patterns. Similarly, widely shared allometry cannot account for forelimb reduction in tyrannosauroids [17]. Furthermore, negative allometry is not observed in giant maniraptoriforms (e.g. *Deinocheirus*; *Therizinosaurus*), which do not display reduced forelimbs and were almost certainly not primarily carnivorous [22,23]. This is in contrast to abelisaurids, carcharodontosaurids and tyrannosaurids, which were strictly carnivorous [24–26]. However, the carnivorous megaraptorids and spinosaurids both also include giant taxa but retain elongated forelimbs [7,8,21], suggesting that a factor other than allometry/body size drove forelimb evolution among theropods.

Here, we provide a novel quantification of forelimb reduction across a broad representation of non-avian theropods in order to investigate potential correlations between this phenomenon and factors including increasing body size, skull size and cranial robusticity. We present and implement a novel scoring methodology that combines *quantitative* and *qualitative* measures of cranial robusticity into a single cranial robusticity index. This cranial robusticity quantification, combined with data on forelimb structure and body mass estimates, is analysed using comparative phylogenetic and other statistical approaches, in order to test potential correlations and trends. We place our results in the wider context of non-avian theropod evolution and evaluate which hypotheses best explain patterns of cranial robusticity, forelimb reduction and gigantism.

2. Methods

(a) Supertree construction

A supertree detailing the interrelationships among 176 non-avian theropods was grafted together from the results of numerous previous analyses (see electronic supplementary material, table S1, for clade definitions). Some taxa that lacked sufficient cranial/forelimb material for use in this study were included in the supertree for calibration purposes, as they were among the earliest members of several key clades (e.g. *Lythronax*; Tyrannosauridae; *Neovenator*; Carcharodontosauridae). Stratigraphic range data for each taxon were taken from the primary literature, based on radiometrically dated horizons where possible. Uncertainty in taxon/formation age was accounted for by treating the data as minimum and maximum ages. The topology was calibrated using the '*paleotree*' package [27] in R v.4.3.1. Stratigraphic data were treated as random observations and branch lengths distributed equally among all branches with minimum branch length set at 1 million years (Ma). This calibration approach follows those of Gates *et al.* [12] and Aubier *et al.* [28]. The topology is provided in electronic supplementary material, S4.

(b) Dataset

Forelimb, cranial and body mass data were collected for 85 non-avian theropod species (electronic supplementary material, S1). Attempts were made to obtain all relevant data for each species from a single specimen to avoid introducing error as a result of size discrepancies among individuals. Where this was not possible, specimens of similar size were used and overlapping elements were scaled to the most complete specimen for analysis (see electronic supplementary information for further details). Cranial data comprised anteroposterior skull lengths (tip of premaxilla to quadrate condyle posterior surface), dorsoventral heights (maximum height excluding cranial crests), dental characteristics, bite force estimates and the degree of fusion between various cranial bones. Forelimb data consisted of absolute proximodistal lengths for the humerus, radius, metacarpal II and each phalanx of digit II (electronic supplementary material, figure S1). The second digit was used because this digit is typically the longest in the theropod manus [29]. In taxa where the second digit was secondarily lost (e.g. Alvarezsauroidea), the first digit was used instead.

Skull–forelimb length ratios (SFR) could be calculated for 61 of the 85 taxa. The SFR provides a measure of forelimb reduction relative to the skull, in that taxa with an SFR ≥ 1.0 are deemed to display reduced forelimbs and those with an SFR ≥ 1.2 are deemed to display vestigial forelimbs. These boundaries are based on observed ratios in taxa where the reduction/vestigiality was first identified (e.g. *Meraxes gigas*, SFR; 1.562 [17]; *Carnotaurus sastrei*, SFR; 1.224 [19]). Despite this, it is likely that the precise results of the current study would change if these boundaries were subtly different (±0.1). To investigate the potential impact of using different SFR thresholds for defining reduced and vestigial forelimbs, two sensitivity analyses were conducted, one with these thresholds set at 0.9 and 1.1, respectively, and one with them set at 1.1 and 1.3, respectively.

(c) Quantifying cranial robusticity

For theropods, cranial robusticity has often been specified by way of morphological comparisons of cranial characters (relative skull height, dental morphology, etc.) [25,26]. Despite the wide range of cranial robusticity observable within Theropoda, a universally applicable method for quantifying this feature, which accounts for dental morphology, skull proportions, bite force and the extent of fusion of individual skull elements, has yet to be formulated. Here, we develop a new method for quantifying the robustness of theropod skulls, considering their particular morphology and attributes. The new method is hereafter termed

the Cranial Robusticity Score (CRS) and quantifies cranial robusticity based on the following characteristics: (i) maximum dorsoventral height-anteroposterior length ratio (DV/AP), (ii) dental morphology, inferred from crown base ratios, (iii) number of fused elements and the degree/likelihood of cranial kinesis, and (iv) bite force estimates inferred from temporal jaw adductor physiological cross-sectional area as a proxy for muscle attachment area. These characters are used here to calculate a CRS ranging from 3 to 50 with a score of 3 representing the lowest possible robusticity and a score of 50 representing the greatest possible robusticity. For taxa that do not preserve sufficient cranial material, the components of the CRS were calculated using the closest relatives available (the bite force of *Tyrannotitan* is based on other giganotosaurin carcharodontosaurids [8323N]). See electronic supplementary material, figure S2, for further details of the CRS.

(d) Missing data

Missing data in palaeontological studies are almost unavoidable [30,31], such that studies have often resorted to estimating data based on closely related species (e.g. [12]). Missing data have been shown to have deleterious effects on various multivariate analyses, because certain data may be unavailable for some of the traits under study [32]. Initial examination showed that a substantial number of data points were missing from the dataset, with over 20% of cells lacking data (289/1245 cells). In order to circumvent this issue and obtain as complete a dataset as possible, the R package '*Rphylopars*' [32] was utilized. We mathematically imputed missing multivariate data points using a restricted maximum likelihood model assuming Brownian motion. To assess the impact of using imputed datasets in analyses, each of the following analyses was conducted with the imputed dataset (ID) as well as the original dataset (OD).

(e) Statistical analyses

To test for relationships between SFR and (i) body size, (ii) body mass, (iii) skull size, and (iv) cranial robusticity (based on CRS), we conducted Spearman's rank correlations and linear regression because our data consist of both continuous and discrete values, for both independent and dependent variables [33]. This was done to establish whether or not the possession of reduced forelimbs is predictable based on aspects of the cranial skeleton and/or absolute body measurements. Body mass data were $\log_{10}$-transformed because the absence of such transformations can have significant impacts on the results of macroevolutionary analyses by increasing the rate of false positives in phylogenetic comparative analyses [34]. Further analyses were conducted with CRS and SFR normalized against the body mass of the taxon in question by taking the residuals of the former two regressed against body mass. Ancestral state estimations for SFR, CRS and body mass were obtained from the '*Rphylopars*' package to track their evolution across Theropoda. Phylogenetic signal tests for the SFR and CRS were conducted using Pagel's λ [32] and Blomberg's K-statistic [35] and tested against null models of evolution assuming Brownian motion. Phylogenetic generalized least squares (PGLS) analyses were conducted in the R package '*picante*' [36] to investigate the possibility of phylogenetic non-independence among the traits under study. CRS, SFR and $\log_{10}$(body mass) were iteratively included in PGLS analyses, and the best-fitting model(s) was identified via size-corrected Akaike information criterion (AICc) scores. Correlation between the residuals of linear models of SFR approximately $\log_{10}$(body mass) and CRS approximately $\log_{10}$(body mass) was tested using PGLS regressions to provide body-mass-corrected estimates for SFR and CRS. All analyses were run with herbivorous and omnivorous taxa (Ornithomimosauria, Therizinosauria, Oviraptorosauria; simply herbivores hereafter) included in the ID and OD datasets and with these taxa excluded in order to explore the phylogenetic and ecological distributions of patterns of forelimb reduction and cranial robusticity. Removing Ornithomimosauria and Oviraptorosauria also permits testing forelimb reduction in the absence of clades which exhibit positive forelimb allometry [21]. We applied a Vuong test to determine if the two possible regression models (x~y versus y~x) are distinct and to identify potential causality between the residuals of the two variables of the best fit PGLS model. For further detail on the analytical procedures and methods used in this work, see electronic supplementary material, S2.

3. Results

(a) Bivariate analyses—Spearman's correlation

All bivariate analyses produced significant positive correlations of varying strengths between skull/forelimb ratio (SFR) and cranial robusticity score (CRS), $\log_{10}$(body mass) and $\log_{10}$(skull size) in both the imputed and non-imputed datasets (electronic supplementary material, table S2, figures S2–S5). Despite the varying strengths of the correlations, all traits are strongly correlated with SFR, with body mass showing a weaker correlation than CRS and skull size. The values of the correlation coefficients of the OD are greater than those of the ID. However, while the correlations appear weaker for the imputed data, the results are still significant for the ID ($p < 0.01$ for all analyses), indicating that the imputation of missing data is unlikely to have introduced an artificial signal/result. When herbivorous taxa are excluded from the analyses, R^2 values for comparisons between all variables increase (0.419–0.684 (SFR~$\log_{10}$(body mass)) and 0.691–0.694 (SFR~CRS) and 0.568–0.684 (SFR~$\log_{10}$(skull size))). This suggests that carnivorous diets are more correlated with greater values of SFR and CRS (i.e. more reduced forelimbs and more robust skulls). When body mass is accounted for, a strong correlation between SFR and CRS and between the residuals of SFR~CRS is observed ($R^2 = 0.520$; $p << 0.001$; figure 1*a*). Similarly, skull size shows a strong correlation with SFR when body mass is accounted for ($R^2 = 0.978$; $p << 0.001$). Therefore, when accounting for the covariant effect of body mass, CRS and skull size are strongly correlated with SFR (figure 1).

(b) Phylogenetic signal—Pagel's λ and Blomberg's K

Pagel's λ and Blomberg's K values for phylogenetic signal of SFR were between 0 and 1 (electronic supplementary material, table S3). Pagel's λ is significantly greater than 0 ($p = 5.52 \times 10^{-17}$) and significantly less than 1 ($p = 9.46 \times 10^{-4}$). This indicates that the datasets used in this study do not fit a Brownian motion model and are therefore not random, suggesting directional selection on SFR and convergence in forelimb reduction among theropod clades. Blomberg's K is also significantly higher than would be expected under a random model (electronic supplementary material, table S3). These values indicate that a significant degree of phylogenetic signal is present in SFR among lineages which possess reduced forelimbs. This demonstrates that phylogenetic position is a relatively good predictor of the extent to which forelimbs are, or are not, reduced/vestigial. When herbivorous taxa are removed from the analysis, both measures of phylogenetic signal increase slightly ($K = 0.7282738$, Pagel's $\lambda = 0.8951$) and remain indicative of a non-random model of forelimb evolution.

(c) Evolution of reduced forelimbs—ancestral state estimation

The evolutionary histories of CRS, SFR and body mass are shown in figure 2. Ancestral estimation and empirical SFR values suggest that reduced forelimbs (SFR ≥ 1.0) evolved in at least five disparate lineages of carnivorous theropods (Abelisauridae, Carcharodontosauridae, Ceratosauridae, Megalosaurinae and Tyrannosauridae; electronic supplementary material, table S4). Reduced forelimbs first appear in abelisauroids (SFR = 1.053) and are reduced further in abelisaurids (SFR = 1.294), in which the forelimb becomes vestigial (SFR ≥ 1.2). Within brachyrostran abelisaurids, the forelimb is reduced even further (SFR = 1.424). *Ceratosaurus* is the only ceratosaurid to possess reduced forelimbs (SFR = 1.022). Reduced forelimbs are also seen in members of Megalosaurinae (SFR = 1.032), but the degree of reduction is slightly less than in abelisauroids. When the threshold for reduction is raised (SFR ≥ 1.1), neither Ceratosauridae nor Megalosaurinae ancestrally possessed reduced forelimbs. However, *Torvosaurus* still meets the threshold for reduction (SFR = 1.118). The carcharodontosaurid ancestor (SFR = 1.027) possessed reduced forelimbs, and giganotosaurin carcharodontosaurids (SFR = 1.530) possessed forelimbs that are even more reduced than those of abelisaurids, although this may be due to the more elongated skull of the former [17]. When applying the higher threshold for reduced forelimbs, only carcharodontosaurids later-diverging than *Concavenator* show the reduced state (SFR = 1.275). Tyrannosaurids possessed ancestrally reduced forelimbs with an ancestral SFR of 1.127, whereas Pantyrannosauria has an ancestral SFR of 0.682; and the greatest degree of forelimb vestigialization in the most derived taxa (*Tyrannosaurus rex*: 1.622). Within Tyrannosauridae, SFR increases from 1.127 to 1.212 in tyrannosaurines and finally to 1.220 in late-diverging tyrannosaurines. Alvarezsauridae do not qualify as possessing reduced forelimbs relative to the skull (SFR = 0.938), although when a lower threshold is applied (SFR ≥ 0.9), the ancestral alvarezsaurid did possess reduced forelimbs. This may be due to the apomorphically small skulls in this clade, which lower the SFR of our sampled alvarezsaurids.

The above patterns largely persist even when alternative definitions of 'reduced' and 'vestigial' forelimbs are used. Regardless of the differing SFR thresholds applied, Tyrannosauridae, later-diverging Abelisauridae and Carcharodontosauridae all possess ancestrally reduced forelimbs, while Megalosaurinae and *Ceratosaurus* do not possess reduced forelimbs using the higher threshold (SFR = 1.028 and 1.066, respectively). Similarly, only Brachyrostra and Giganotosaurini possess vestigial forelimbs at all thresholds, while Tyrannosaurinae are inferred to possess vestigial forelimbs at the lower and middle thresholds. However, SFR values between early-diverging (*Dynamoterror* SFR = 1.296) and later-diverging Tyrannosaurinae (*Daspletosaurus* SFR = 1.09; *Tyrannosaurus* SFR = 1.622) imply that vestigial forelimbs evolved in the tyrannosaurine ancestor, and the forelimbs may have secondarily increased in size in *Daspletosaurus*.

(d) Phylogenetic generalised least squares

Significant correlations between SFR, CRS, $\log_{10}$(skull size) and $\log_{10}$(body mass) (electronic supplementary material, tables S5 and S6) were recovered, albeit much weaker than that calculated in the Spearman's correlation tests. Corrected Akaike information criterion (AICc) scores demonstrate that the best-fit model to describe SFR includes CRS and body mass, with the second-best model including CRS and skull size. Therefore, large body size and high cranial robusticity seem to influence forelimb reduction relative to the skull. No phylogenetic outliers were detected based on the standard for determining outliers via the value of phylogenetic residuals (≥ 3) [37]. The AICc scores can be assessed using the following likelihood test [38] (equation 3.1).

$$\theta = \exp\left(\frac{\mathrm{AICc}_x - \mathrm{AICc}_y}{2}\right). \tag{3.1}$$

θ = Likelihood of model AICc_y relative to AICc_x, AICc_n = AICc of nth model

Using equation (3.1), the model including CRS and body mass substantially outperforms all other models (electronic supplementary material, tables S5 and S6). When herbivorous taxa are removed, correlations between SFR and all variables increase (electronic supplementary material, tables S7 and S8), further suggesting that the correlations are stronger within carnivorous taxa. The best-fit model includes CRS and body mass. The second-best model only includes CRS, showing that CRS is the single best explanatory predictor for forelimb reduction, although maximum variation is explained when body mass is included. When the residuals between the models CRS~body mass and SFR~body mass were tested (SFR~CRS), a significant correlation between them is observed both when herbivorous taxa are included ($R^2 = 0.289$; $p = 1.598 \times 10^{-7}$; AICc = −30.01;

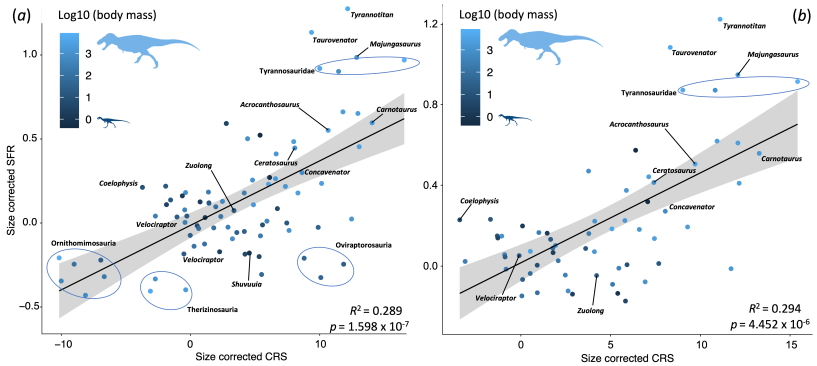

Figure 1. Results of PGLS regression of the residuals of SFR and CRS corrected for body mass including (*a*) and excluding (*b*) herbivorous taxa, with select taxa highlighted. Silhouettes are by S. Hartman, from phylopic.org and used under a Creative Commons License (CC BY 3.0).

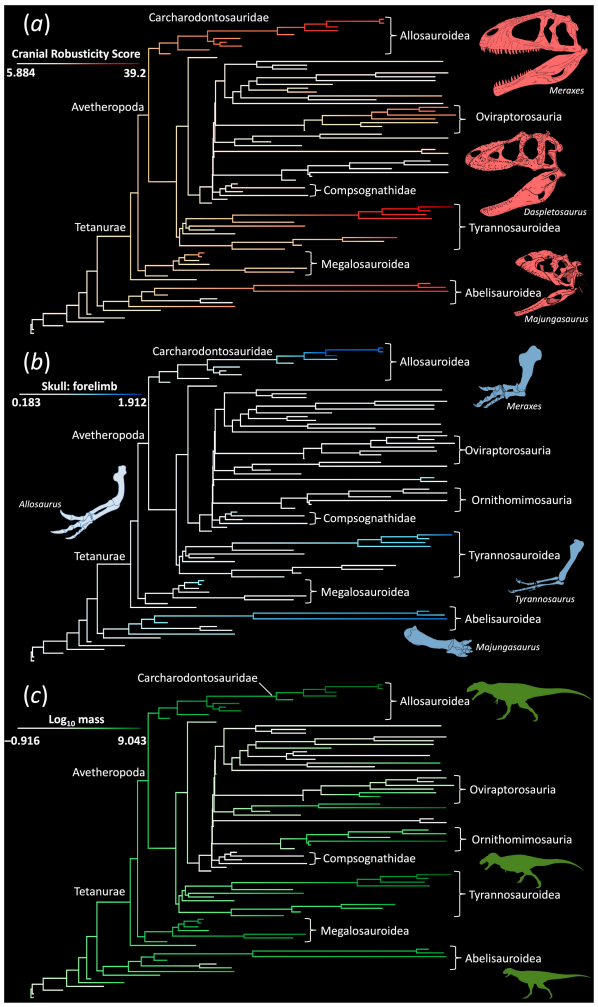

Figure 2. Phylogenetic heat maps of the traits considered in this work. Cranial Robusticity Score (*a*), Skull : Forelimb Ratio (*b*) and log_{10} body mass (*c*). Note that increased cranial robusticity and body mass always precede increases in SFR. Skull silhouettes: *Meraxes gigas* (Eotyrannu5; https://creativecommons.org/licenses/by-sa/4.0 (CC BY-SA 4.0), colour changed to red), *Majungasaurus* (Jaime Headden; https://qilong.wordpress.com/2011/10/19/walking-sledgehammers/; CC BY 3.0; colour changed to red) and *Daspletosaurus*; other silhouettes as in figure 1.

electronic supplementary material, table S6) and excluded (R^2 = 0.2939; p = 4.452 × 10^{-5}, AICc = −25.13; electronic supplementary material, table S8). Our Vuong test shows that the CRS~SFR and SFR~CRS models are distinct from each other (ω^2 = 0.578; p = 1.02 × 10^{-5}) and that SFR is most likely a function of CRS as opposed to *vice versa* (z = 34.551; p = 2 × 10^{-16}).

4. Discussion

(a) Patterns and trends in forelimb reduction

Reduced forelimbs, defined by an SFR ≥ 1.0 (skull length ≥ forelimb length), evolved independently in at least five carnivorous theropod lineages which occupy disparate positions within non-avian theropod phylogeny: Abelisauridae, Carcharodontosauridae, Ceratosauridae, Megalosauridae and Tyrannosauridae. Only abelisaurids [19], carcharodontosaurids [17] and tyrannosaurids [14,39] have been previously identified as possessing the reduced condition. Within these three clades, vestigial forelimbs, defined by an SFR ≥ 1.2 (skull length ≥ forelimb length × 1.2), eventually appear during their evolution. This demonstrates that the reduction of the forelimb was a relatively common trend across Theropoda, suggesting that similar ecological/evolutionary pressures governed the trends seen in forelimb evolution. Below, evolutionary trends relating to the forelimbs of each group are described in detail utilizing the ancestral estimates and values in electronic supplementary material, S1.

In the early-branching abelisauroid *Eoabelisaurus*, the forelimb is similar in its proportions to those of other early-diverging theropods (e.g. *Dilophosaurus*, *Ceratosaurus*) [40] with the exception of the manual skeleton, which is already much reduced. This has previously been used to suggest a stepwise model for abelisauroid forelimbs, starting with modification of the manus [41]. This is supported by later-branching abelisaurids, such as *Majungasaurus* and *Carnotaurus*: these taxa have proportionally larger humeri relative to their forelimbs when compared with the antebrachium and manus in all other abelisaurids, with manual elements among the most reduced/absent forelimb elements compared with *Eoabelisaurus* (electronic supplementary material, table S9). There are distinct differences between the forelimbs of *Majungasaurus* and *Carnotaurus*. *Carnotaurus* (SFR = 1.224) possesses an intermediate stage of forelimb reduction between *Eoabelisaurus* (SFR = 1.12) and *Majungasaurus* (SFR = 1.613). *Majungasaurus* possesses the most reduced forelimbs of any known abelisaurid (SFR = 1.613) and also has the proportionally smallest antebrachium and manus amongst late-diverging abelisauroids. This corroborates previous work which showed that the abelisauroid forelimb was reduced first by shortening the distal elements, and then by slightly shortening the proximal forelimb elements [41]. Compared with other gigantic theropods (e.g. Carcharodontosauridae, Tyrannosauridae), *Majungasaurus* and *Carnotaurus* possess the smallest proportional values for many elements of the forelimb, indicating that the reduction of the forelimb in later-branching abelisaurids was perhaps the most extreme among gigantic carnivores. This is possibly due to the much longer evolutionary history of abelisaurids (179–66 Ma) compared with carcharodontosaurids (155–89 Ma) and tyrannosaurids (81–66 Ma). However, the forelimbs of carcharodontosaurids and tyrannosaurids exhibit similar degrees of reduction in the most extreme cases, suggesting that the degree of reduction is constrained by developmental pathways rather than the time allowed for reduction to occur. More complete remains of abelisaurids intermediate between *Eoabelisaurus* and *Majungasaurus* are needed to determine the tempo of this clade's forelimb evolution in greater detail.

Ceratosaurus also possesses reduced forelimbs with proportions similar to those of early-diverging abelisauroids but with proportions similar to early abelisaurids (electronic supplementary material, table S9). As in early-diverging abelisaurids (*Eoabelisaurus*), forelimb reduction is limited to the manus in *Ceratosaurus*, the phalanges and metacarpals being proximodistally shortened [40]. Despite this, *Ceratosaurus* is not classified as a gigantic theropod, although mass estimates (966 kg) place it very close to the 1000 kg threshold for gigantism. However, it is likely that other *Ceratosaurus* specimens are larger than those used in this work, or the mass of this taxon was slightly underestimated. Indeed, Sombathy *et al.* [42] estimated a mass of 1132 kg for a large *Ceratosaurus* individual (UMNH VP 5278; see electronic supplementary material, S2, for institutional abbreviations), indicating that the individual used in the current study (USNM 4735) may not have been fully grown [42] and may have had a body mass smaller than that used here (702 kg [42]). The presence of reduced forelimbs in *Ceratosaurus* individuals that do not meet the gigantism threshold used here may be attributed to the forelimbs being proportionally small in immature *Ceratosaurus*. This is seen in the tyrannosaurid *Gorgosaurus*, where the reduced forelimbs are present in juveniles as small as 335 kg [43]. Therefore, the presence of reduced limbs is not limited to adult individuals of a species, and so the use of potentially subadult individuals of *Ceratosaurus* in this study is unlikely to have resulted in underestimation of the degree of forelimb reduction for this taxon. As such, it is likely that the initial reduction of the manus occurred near the base of Ceratosauria and became much more apparent in early-diverging abelisauroids and *Ceratosaurus* in association with the evolution of ceratosaurian gigantism.

Unfortunately, most megalosaurid forelimbs are unknown due to the fragmentary nature of the hypodigms of many taxa [44], making evolutionary trends difficult to discern. Despite this, the SFR values obtained for some megalosaurines demonstrate that members of this clade also possessed reduced forelimbs relative to the skull. Compared with other megalosaurids, such as *Afrovenator*, *Torvosaurus* possessed a similarly sized humerus and manus but had a much smaller radius. As a result, the forelimb lengths of *Afrovenator* and *Torvosaurus* are very similar (< 1 cm difference) while the body mass and skull length are much greater in the latter (electronic supplementary material, S1). Baryonychine spinosaurids (*Baryonyx*, *Suchomimus*) were also gigantic to super-gigantic and yet possessed non-reduced forelimbs (SFR: 0.736, 0.753). The SFR of the ancestral megalosauroid is estimated at 0.777, indicating that spinosaurid forelimbs were only slightly reduced relative to the plesiomorphic state. The comparatively low SFR values seen in baryonychines, and probably spinosaurids generally, reflect simultaneous elongation of the skull and forelimbs likely resulting from a degree of limited piscivorous adaptation that left them still capable of hunting a wide range of prey [45,46].

The only allosauroids found to possess reduced forelimbs are the Carcharodontosauridae. Non-carcharodontosaurids, such as *Allosaurus*, possessed SFR values ranging from 0.813 to 0.892, compared with 0.914–1.923 in carcharodontosaurids. If we exclude the smallest carcharodontosaurid, *Concavenator* (670 kg), the SFR range is 1.191–1.923. Giganotosaurin SFRs range from 1.562 to 1.923 (electronic supplementary material, S8). This demonstrates a clear trend in reduction and vestigialization of the forelimb from early-diverging to derived carcharodontosaurids, in concert with major body mass increases. The proximal and distalmost elements of the carcharodontosaurid forelimb are similar in proportions to those of early-diverging allosauroids,

whereas the forearm is much more reduced (electronic supplementary material, table S10). For example, the proportional lengths of the humerus of *Allosaurus fragilis* and *Acrocanthosaurus* are similar (34–35% forelimb length, respectively), while their radii differ by 4% forelimb length, indicating that antebrachial proportions differ between early-diverging and derived allosauroids [20]. Giganotosaurin carcharodontosaurids also display proportional differences relative to early-diverging carcharodontosaurids. The humeri increase as a proportion of the forelimb between *Acrocanthosaurus* and *Tyrannotitan*. *Meraxes* and *Taurovenator* demonstrate that the giganotosaurin manual skeleton was also reduced compared with that of early-diverging carcharodontosaurids, with the manus being substantially proportionally shorter in giganotosaurins [20] (34% in Giganotosaurini versus 44% in *Allosaurus*; electronic supplementary material, table S10). Therefore, carcharodontosaurid forelimbs evolved in a similar modular fashion to those of abelisaurids, although the initial reduction involved the antebrachium and the later phase involved the manual skeleton [17,20].

Tyrannosauroids show perhaps the clearest trend in forelimb reduction due to the relatively large amount of material pertaining to the forelimbs known for taxa occupying various phylogenetic positions. Early-diverging tyrannosauroids such as *Guanlong* (SFR = 0.548) and *Eotyrannus* (SFR = 0518) possess unreduced forelimbs, most similar to the ancestral coelurosaurian condition (0.645), while larger, later-branching taxa possess shorter forelimbs (*Yutyrannus*: 0.843). SFR in early tyrannosaurids such as *Gorgosaurus* (77–75.6 Ma; SFR = 1.286) and early tyrannosaurines such as *Dynamoterror* (78 Ma; SFR = 1.295) and *Daspletosaurus* (77–74.4 Ma; SFR = 1.09) are considerably lower than in *Tyrannosaurus* (68–66 Ma; SFR = 1.622), indicating relatively rapid forelimb reduction during the middle Campanian–Maastrichtian (figures 2 and 3). The elements of the tyrannosauroid forelimb appear to have initially been reduced in equal proportions, with each element becoming smaller over time. This trend changes with the evolution of the tyrannosaurid manus, where the latter contributes a decreased proportion of forelimb length. The humeri of early-diverging tyrannosauroids are absolutely larger than those of later-diverging forms, as *Yutyrannus* (35.8 cm; 33.3% forelimb length) has a humerus larger than *Gorgosaurus* (32.4 cm; 42.2% forelimb length), despite the latter having a much larger body size. Smaller tyrannosauroids, such as *Guanlong*, possess smaller humeri, similar in proportion to those of other early-diverging forms (23.8 cm; 34.1% forelimb length). In *Daspletosaurus* (35.7 cm; 37.4% forelimb length), the humerus is of comparable absolute length to that of *Yutyrannus*, while the former is at least twice as massive (2840 kg) as the latter (1414 kg). In *Tyrannosaurus*, the humerus is absolutely larger than that of any other tyrannosauroid (length = 38.5 cm; 44.4% forelimb length). This shows that in later-branching tyrannosauroids, the humerus constitutes an increasing proportion of the forelimb. The forearm of tyrannosauroids exhibits drastic differences in size and proportion during its evolution, with tyrannosaurids (*Gorgosaurus*; 20.3% forelimb length; *Daspletosaurus*; 17.9%; *Tyrannosaurus*; 19.9%) showing much shorter radii (and ulnae) than small (*Eotyrannus*; 31.1% forelimb length) and gigantic (*Yutyrannus*; 25.4% forelimb length) non-tyrannosaurids. Furthermore, the forearms of smaller tyrannosauroids, such as *Tanycolagreus* (22.4%) and *Guanlong* (22.9%) are proportionally larger than those of the large-bodied tyrannosaurids. The manus changes from being 123% (*Yutyrannus*) or 126% (*Guanlong*) the length of the humerus in early tyrannosauroids to 136% in intermediate tyrannosauroids (*Eotyrannus*) and 119% (*Daspletosaurus*) and 80% (*Tyrannosaurus*) in tyrannosaurines. Thus, each portion of the tyrannosaurid forelimb became gradually reduced in approximate synchrony (electronic supplementary material, table S11), with no element(s) clearly becoming reduced before any other(s), unlike the more modular pattern observed in abelisauroids and allosauroids.

One potential caveat concerning the evolution of tyrannosaurid forelimbs is that one tyrannosaurid subclade, Alioramini, is characterized by longirostrine skulls, gracile proportions and lower body mass compared with tyrannosaurines [24,47]. Alioramins probably differed in their hunting style from other tyrannosaurids, with the former specializing in small, agile prey items [48–50]. However, the alioramin body plan likely evolved secondarily from the body plan of other later-diverging tyrannosauroids given that alioramins are phylogenetically bracketed by large-bodied taxa with robustly built skulls [51–54].

Although our results do not fully support forelimb reduction in alvarezsaurians, this is probably attributable to the following: (i) the relatively small skulls of alvarezsaurids, (ii) the trend towards miniaturization observed in Alvarezsauria [55], and (iii) the highly specialized ecology of derived alvarezsaurians, which are hypothesized to have been insectivores adapted to digging [56,57]. The fact that alvarezsaurians do not meet the thresholds for forelimb reduction may be explained by miniaturization, possibly as an adaptation for their insectivorous lifestyles, constraining the level of forelimb reduction relative to the skull. This is supported by the role that CRS and body mass play in the evolution of reduced forelimbs in carnivorous theropods. Therefore, although the forelimbs of alvarezsaurians were reduced throughout their evolution, their reduction was probably related to their use in prey acquisition [57]. In short, alvarezsaurian forelimb reduction is likely not analogous to forelimb reduction in gigantic theropods, but was driven by their distinct ecology.

(b) Drivers of forelimb reduction

Our analyses demonstrate that the presence of reduced/vestigial forelimbs is significantly correlated with cranial robusticity and is associated with body mass increases towards gigantism and super-gigantism whilst displaying a relatively high degree of phylogenetic signal (figure 1, electronic supplementary material, figures S5 and S6; tables S2 and S3). Among the correlations tested, those including cranial robusticity are shown to be most significant, although they appear weaker when accounting for phylogenetic relationships. Therefore, cranial robusticity increases were probably the primary driver of forelimb reduction, with body mass as a likely accessory driver. The subsidiary role of body mass is supported by the observation that some taxa have very high CRS and SFR values but do not exhibit commensurately large body mass, such as *Majungasaurus* (SFR = 1.613; body mass = 1614 kg), *Taurovenator* (SFR = 1.781; body mass = 5728 kg) and *Tyrannosaurus* (SFR = 1.622; body mass = 8462 kg) (figures 2 and 3). Thus, the reduction of the forelimb in gigantic theropods is not primarily driven by allometric growth, contrary to some previous studies [17,21]. Instead, the 'allometric' signal may have been driven by the increases in cranial

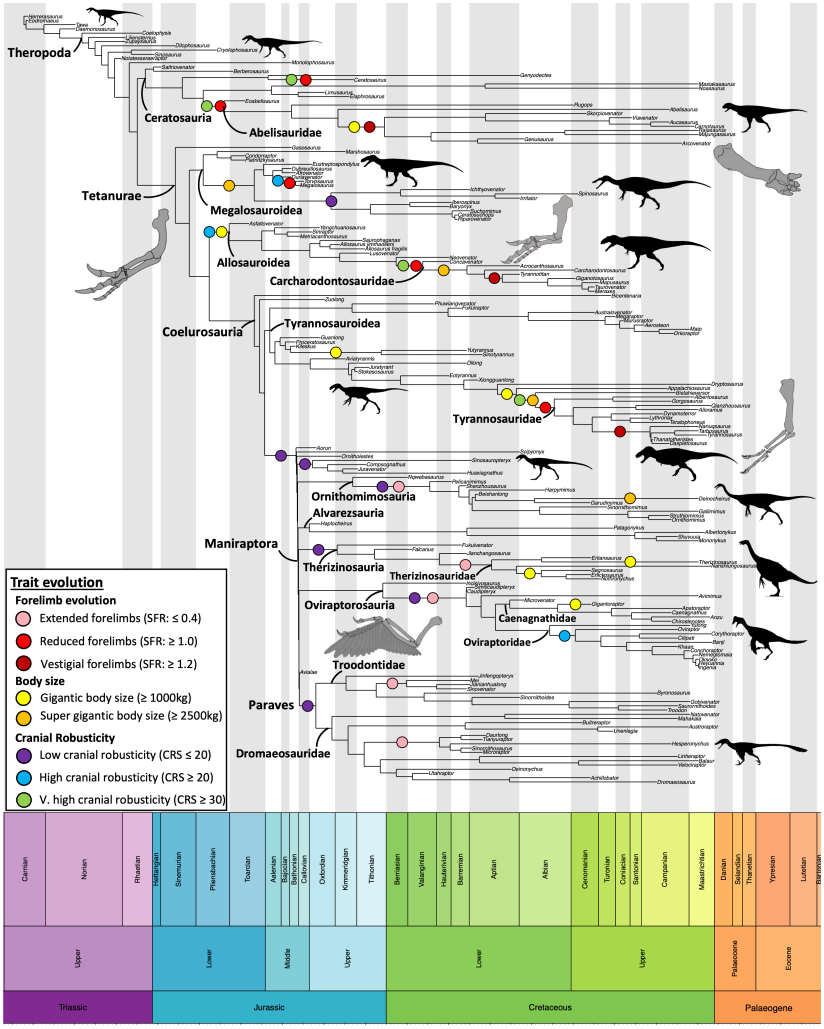

Figure 3. The evolution of cranial robusticity, forelimb proportions and body mass in each major theropod clade considered in this work. Trait optimization based on ancestral state estimation and absolute values for terminal taxa. Note the convergent evolution of reduced forelimbs, high cranial robusticity and gigantic body size in primarily hypercarnivorous clades. Silhouettes by S. Hartman, available from phylopic.org and used under a Creative Commons license (CC BY-NC-SA 3.0).

robusticity leading to forelimb reduction, which is supported by the significant correlation we find between CRS and body mass ($p = 2.488 \times 10^{-7}$). Indeed, Palma Liberona *et al.* [21] found that Oviraptorosauria and Ornithomimosauria did not demonstrate the negative forelimb allometry found in other theropod clades such as Allosauroidea and Tyrannosauroidea. Here, we find that oviraptorosaurians and ornithomimosaurians do not possess reduced forelimbs or, with some exceptions, gigantic body sizes. Ornithomimosaurians also lack highly robust crania. These clades are also highly ecologically distinct relative to gigantic allosauroid and tyrannosauroid theropods. As such, it is probable that ecological factors drove forelimb reduction in gigantic predators, as opposed to negative allometry associated with body mass increases.

The biological drivers of increasing cranial robusticity, and the role of general diet specifically, have been investigated in several extant tetrapod clades, with prey size being particularly significant in carnivores and plant food properties being significant in herbivores. It has been suggested that increased skull robusticity and body size correlates with larger prey size in toothed whales [58], which are analogous to theropods in that prey capture involves the jaws rather than the forelimbs. Similar patterns are also seen in numerous other tetrapod groups, including Rodentia, Lepidosauria and Crocodylomorpha [59–61]. While rodents may vary their skull construction according to plant type [60], lepidosaurs and crocodylomorphs vary their skull robustness according to prey type and size [59,61]. Extending this linkage between cranial robusticity and prey choice to theropod dinosaurs is plausible, given that skull shape and degree of fusion between elements has been shown to have affected cranial performance in some theropod groups and impacted the composition of the predators' diet [62,63]. Therefore, it is highly likely that a predator's cranial robusticity was linked to the characteristics of the organisms it was preying upon. Larger prey items would have required a larger, more robust skull to resist the inevitably higher forces experienced when attacking/restraining heavier prey.

The existence of large-bodied prey items, which lived alongside theropods throughout the Mesozoic, likely resulted in certain theropod lineages growing to gigantic sizes. Given that theropod gigantism is linked with more robust crania and reduced forelimbs, as well as the predator–prey body size relationships observed across tetrapods [43,64,65], it is probable that gigantic theropods were specialized to hunt large-bodied prey, which required larger body size and higher cranial robusticity to subdue [66,67]. This specialization resulted in a shift away from using the forelimb in prey capture towards a jaw-based approach, ultimately resulting in the loss of the forelimbs' role in hunting and eventually their reduction/vestigialization. All taxa studied here which possess robust skulls (CRS ≥ 30) are known to have coexisted with a variety of megaherbivore

taxa, both larger and smaller than the predator. This trend persisted throughout the latter half of the Mesozoic and across all continents [68–75]. For example, in Late Jurassic North America (approximately 156 to approximately 146 Ma), *Allosaurus* and *Torvosaurus* coexisted with gigantic sauropods, as well as large thyreophorans and ornithopods, with abundant evidence for a predator–prey relationship between the theropods and megaherbivores [68,69]. In the Early Cretaceous (approximately 112–89 Ma) South America, numerous giganotosaurins lived alongside the largest known titanosaurian sauropods [17,70]. Due to numerous adaptations in the skull which enabled giganotosaurins to produce much stronger bite forces, combined with probable pack behaviour [70], it is likely that they preyed on juvenile individuals of these titanic sauropods [72]. Additionally, Late Cretaceous North America (81–66 Ma) hosted an array of tyrannosaurids which coexisted with numerous large hadrosaurids and ceratopsids [73–75].

The common and persistent co-occurrence of numerous super-gigantic theropods and megaherbivores suggests that a predator–prey arms race [76,77] drove increasing cranial robusticity and body sizes in these theropods. Our findings align well with this hypothesis. The increased body size of the potential prey items for these theropods would have likely resulted in the necessity for a stronger bite in order to capture and restrain larger juveniles. This would then lead to an increase in the body size of the predator. Therefore, the most likely drivers of forelimb reduction are primarily increased cranial robusticity and body size in response to the increased body size of their potential prey items. This evolutionary arms race suggests that the selection pressure leading to forelimb reduction was related to the increasing redundancy of these structures in prey capture, leading to their reduction for energetic benefits.

It should be noted that while we have demonstrated a clear correlation between CRS and SFR, the above scenario does not preclude forelimb reduction also influencing cranial robusticity. However, despite the results showing no direction of causality between the two variables, it is more plausible that the reason for the correlations observed is increasing cranial robusticity. The inverse relationship—forelimb reduction driving increasing robusticity implies that the forelimbs responded more directly to an environmental pressure, which resulted in their reduction. While we do not disregard the plausibility of this scenario, it predicts the existence of predators with reduced forelimbs and relatively low cranial robusticity, which would be a less efficient strategy for prey capture than increasing cranial robusticity prior to forelimb reduction [26]. Our Vuong test shows that SFR is most likely a function of CRS, supporting the conclusion that forelimb reduction is driven by cranial robusticity. Although the R^2 for the relationship between CRS and SFR appears relatively low, the effect size ($R = 0.537$) is large, meaning that while the power of the SFR to accurately predict CRS is low, the latter explains a large part of the variance in SFR [78]. Furthermore, ancestral state reconstructions indicate that increases in CRS and body mass beyond their respective thresholds always precede increases in SFR (figures 2 and 3), suggesting that reduction/vestigialization of the forelimb is a function of cranial robusticity and, secondarily, body mass. The relationship between cranial robusticity and forelimb reduction identified here leads us to hypothesize that the forelimbs became reduced due to their redundancy as the head took on the leading role in prey capture among gigantic carnivores. For discussion of developmental mechanisms of forelimb reduction, see electronic supplementary material, S2.

5. Conclusion

We have shown that reduced forelimbs evolved in at least five disparate non-avian theropod clades, with each displaying different reduction patterns. These disparate patterns highlight the convergent nature of forelimb reduction and demonstrate that organisms may find different ways to adapt [79] to common selection pressures and that no single genetic mechanism can be invoked to explain the reduction observed. Forelimb size relative to the skull is significantly correlated with cranial robusticity and body mass, whereas body mass and skull size alone are not, suggesting that high cranial robusticity was the primary driver of forelimb reduction. Although secondary, body mass increases were driven by increasing prey body size. We postulate that forelimb reduction was a product of their redundancy in prey capture in these large theropods, whereas the elongate forelimbs observed in the smaller maniraptoriformes are consistent with a distinct grasping predation style suitable for tackling smaller prey. Elongate forelimbs may be related to the evolution of pennaceous feathers, and probably flight [80,81], or perhaps reliance on the forelimb rather than the skull in prey capture in spinosaurids [46] and megaraptorids [82]. Future work should aim to answer this question of limb function in maniraptoriformes as it will aid in our understanding of the significance of the forelimb in the evolution of feathers (and flight) in non-avian dinosaurs. Further insights may also come from combining the CRS with data from other approaches, such as three-dimensional geometric morphometrics and finite element analyses, to more thoroughly analyse forelimb evolution among theropods.

Ethics. This work did not require ethical approval from a human subject or animal welfare committee.

Data accessibility. All data and R code used in this study are available in the electronic supplementary information [83].

Declaration of AI use. We have not used AI-assisted technologies in creating this article.

Authors' contributions. C.R.S.: conceptualization, data curation, formal analysis, investigation, methodology, visualization, writing—original draft, writing—review and editing; E.S.: methodology, visualization, writing—original draft, writing—review and editing; P.U.: conceptualization, methodology, project administration, supervision, validation, writing—original draft, writing—review and editing.

All authors gave final approval for publication and agreed to be held accountable for the work performed therein.

Conflict of interest declaration. We declare we have no competing interests.

Funding. E.M.S. is supported by a Sarah Woodhead Research Fellowship in Earth Sciences (Girton College, Cambridge).

Acknowledgements. This study formed C.R.S.'s MSc thesis carried out at University College London in 2023–2024. We thank G. Funston for insights into the evolution of the tyrannosaurid forelimb. We thank Mauro Aranciaga Rolando and one anonymous reviewer for comments which greatly improved this manuscript.

References

1. Martinez RN, Sereno PC, Alcober OA, Colombi CE, Renne PR, Montañez IP, Currie BS. 2011 A basal dinosaur from the dawn of the dinosaur era in southwestern Pangaea. *Science* **331**, 206–210. (doi:10.1126/science.1198467)
2. Carrano MT, Benson RBJ, Sampson SD. 2012 The phylogeny of *Tetanurae* (Dinosauria: Theropoda). *J. Syst. Palaeontol*. **10**, 211–300. (doi:10.1080/14772019.2012.713753)
3. Brusatte SL, O'Connor JK, Jarvis ED. 2015 The origin and diversification of birds. *Curr. Biol*. **25**, R888–98. (doi:10.1016/j.cub.2015.08.003)
4. Wills S, Underwood CJ, Barrett PM. 2023 Machine learning confirms new records of maniraptoran theropods in Middle Jurassic UK microvertebrate faunas. *Pap. Palaeontol*. **9**, e1487. (doi:10.1002/spp2.1487)
5. Tykoski RS, Rowe T. 2004 Ceratosauria. In *The Dinosauria* (eds D Weishampel, P Dodson, H Osmólska), pp. 47–70, 2nd edn. Berkeley, CA: University of California Press.
6. Sorkin B. 2021 Scansorial and aerial ability in *Scansoriopterygidae* and basal *Oviraptorosauria*. *Hist. Biol*. **33**, 3202–3214. (doi:10.1080/08912963.2020.1855158)
7. Fabbri M *et al*. 2022 Subaqueous foraging among carnivorous dinosaurs. *Nature* **603**, 852–857. (doi:10.1038/s41586-022-04528-0)
8. Sereno PC, Myhrvold N, Henderson DM, Fish FE, Vidal D, Baumgart SL, Keillor TM, Formoso KK, Conroy LL. 2022 Spinosaurus is not an aquatic dinosaur. *eLife* **11**, e80092. (doi:10.7554/elife.80092)
9. Dyke G, de Kat R, Palmer C, van der Kindere J, Naish D, Ganapathisubramani B. 2013 Aerodynamic performance of the feathered dinosaur Microraptor and the evolution of feathered flight. *Nat. Commun*. **4**, 2489. (doi:10.1038/ncomms3489)
10. Pei R *et al*. 2020 Potential for powered flight neared by most close avialan relatives, but few crossed its thresholds. *Curr. Biol.* **30**, 4033–4046. (doi:10.1016/j.cub.2020.06.105)
11. Benson RBJ, Campione NE, Carrano MT, Mannion PD, Sullivan C, Upchurch P, Evans DC. 2014 Rates of dinosaur body mass evolution indicate 170 million years of sustained ecological innovation on the avian stem lineage. *PLoS Biol*. **12**, e1001853. (doi:10.1371/journal.pbio.1001853)
12. Gates TA, Organ C, Zanno LE. 2016 Bony cranial ornamentation linked to rapid evolution of gigantic theropod dinosaurs. *Nat. Commun*. **7**, 12931. (doi:10.1038/ncomms12931)
13. Hendrickx C, Hartman S, Mateus O. 2015 An overview of non-avian theropod discoveries and classification. *PalArch's J. Vertebr. Palaeontol*. **12**, 1–73.
14. Lambe LM. 1914 On a new genus and species of carnivorous dinosaur from the Belly River Formation of Alberta, with a description of *Stephanosaurus marginatus* from the same horizon. *Ott. Nat*. **28**, 13–20.
15. Burch SH. 2017 Myology of the forelimb of *Majungasaurus crenatissimus* (Theropoda, Abelisauridae) and the morphological consequences of extreme limb reduction. *J. Anat*. **231**, 515–531. (doi:10.1111/joa.12660)
16. Guinard G. 2020 Forelimb shortening of *Carcharodontosauria* (Dinosauria: Theropoda): an update on evolutionary anterior micromelias in non-avian theropods. *Zoology* **139**, 125756. (doi:10.1016/j.zool.2020.125756)
17. Canale JI *et al*. 2022 New giant carnivorous dinosaur reveals convergent evolutionary trends in theropod arm reduction. *Curr. Biol.* **32**, 3195–3202. (doi:10.1016/j.cub.2022.05.057)
18. Osborn HF. 1905 *Tyrannosaurus* and other carnivorous dinosaurs. *Bull. Am. Mus*. **21**, 259–265.
19. Bonaparte JF, Novas FE, Coria RA. 1990 *Carnotaurus sastrei* Bonaparte, the horned, lightly built carnosaur from the Middle Cretaceous of Patagonia. *Contrib. Sci*. **416**, 1–41. (doi:10.5962/p.226819)
20. Aranciaga Rolando AM, Motta MJ, Agnolín FL, Tsuihiji T, Miner S, Brissón-Egli F, Novas FE. 2024 A new carcharodontosaurid specimen sheds light on the anatomy of South American giant predatory dinosaurs. *Sci. Nat*. **111**, 56. (doi:10.1007/s00114-024-01942-4)
21. Palma Liberona JA, Soto-Acuña S, Mendez MA, Vargas AO. 2019 Assesment and interpretation of negative forelimb allometry in the evolution of non-avian Theropoda. *Front. Zool*. **16**, 44. (doi:10.1186/s12983-019-0342-9)
22. Barrett PM. 2005 The diet of ostrich dinosaurs (Theropoda: Ornithomimosauria). *Palaeontology* **48**, 347–358. (doi:10.1111/j.1475-4983.2005.00448.x)
23. Zanno LE, Makovicky PJ. 2011 Herbivorous ecomorphology and specialization patterns in theropod dinosaur evolution. *Proc. Natl Acad. Sci. USA* **108**, 232–237. (doi:10.1073/pnas.1011924108)
24. Lü J, Xu L, Pu H, Jia S, Azuma Y, Chang H, Zhang J. 2014 Paleogeographical significance of carcharodontosaurid teeth from the late Early Cretaceous of Ruyang, Henan Province of central China. *Hist. Biol.* **25**, 1–6. (doi:10.1080/08912963.2014.947287)
25. Ma W, Pittman M, Butler RJ, Lautenschlager S. 2022 Macroevolutionary trends in theropod dinosaur feeding mechanics. *Curr. Biol*. **32**, 677–686. (doi:10.1016/j.cub.2021.11.060)
26. Pereyra EES, Vrdoljak J, Ezcurra MD, González-Dionis J, Paschetta C, Méndez AH. 2025 Morphology of the maxilla informs about the type of predation strategy in the evolution of *Abelisauridae* (Dinosauria: Theropoda). *Sci. Rep*. **15**, 7857. (doi:10.1038/s41598-025-87289-w)
27. Bapst DW. 2012 paleotree: an R package for paleontological and phylogenetic analyses of evolution. *Methods Ecol. Evol*. **3**, 803–807. (doi:10.1111/j.2041-210X.2012.00223.x)
28. Aubier P, Jouve S, Schnyder J, Cubo J. 2023 Phylogenetic structure of the extinction and biotic factors explaining differential survival of terrestrial notosuchians at the Cretaceous–Palaeogene crisis. *Palaeontology* **66**, e12638. (doi:10.1111/pala.12638)
29. Xu X *et al*. 2015 A bizarre Jurassic maniraptoran theropod with preserved evidence of membranous wings. *Nature* **521**, 70–73. (doi:10.1038/nature14423)
30. Kearney M, Clark JM. 2003 Problems due to missing data in phylogenetic analyses including fossils: a critical review. *J. Vertebr. Paleontol*. **23**, 263–274. (doi:10.1671/0272-4634(2003)023[0263:PDTMDI]2.0.CO;2)
31. Wiens JJ. 2003 Incomplete taxa, incomplete characters, and phylogenetic accuracy: is there a missing data problem? *J. Vertebr. Paleontol*. **23**, 297–310. (doi:10.1671/0272-4634(2003)023[0297:iticap]2.0.co;2)
32. Goolsby EW, Bruggeman J, Ané C. 2017 Rphylopars: fast multivariate phylogenetic comparative methods for missing data and within-species variation. *Methods Ecol. Evol*. **8**, 22–27. (doi:10.1111/2041-210x.12612)
33. Chatterjee S, Hadi AS. 2015 *Regression analysis by example*. Hoboken, NJ: John Wiley & Sons.
34. Benson RBJ, Godoy P, Bronzati M, Butler RJ, Gearty W. 2022 Reconstructed evolutionary patterns for crocodile-line archosaurs demonstrate impact of failure to log-transform body size data. *Commun. Biol*. **5**, 171. (doi:10.1038/s42003-022-03071-y)
35. Blomberg SP, Garland T, Ives AR. 2003 Testing for phylogenetic signal in comparative data: behavioral traits are more labile. *Evolution* **57**, 717–745. (doi:10.1111/j.0014-3820.2003.tb00285.x)

36. Kembel SW, Cowan PD, Helmus MR, Cornwell WK, Morlon H, Ackerly DD, Blomberg SP, Webb CO. 2010 Picante: R tools for integrating phylogenies and ecology. *Bioinformatics* **26**, 1463–1464. (doi:10.1093/bioinformatics/btq166)
37. Jones KE, Purvis A. 1997 An optimum body size for mammals? Comparative evidence from bats. *Funct. Ecol*. **11**, 751–756. (doi:10.1046/j.1365-2435.1997.00149.x)
38. Burnham KP, Anderson DR. 2002 *Model selection and multimodel inference: a practical information-theoretic approach*, 2nd edn. New York, NY: Springer.
39. Brochu CA. 2003 Osteology of *Tyrannosaurus rex*: insights from a nearly complete skeleton and high-resolution computed tomographic analysis of the skull. *J. Vertebr. Paleontol*. **22**, 1–138. (doi:10.1080/02724634.2003.10010947)
40. Carrano MT, Choiniere J. 2016 New information on the forearm and manus of *Ceratosaurus nasicornis* Marsh, 1884 (Dinosauria, Theropoda), with implications for theropod forelimb evolution. *J. Vertebr. Paleontol*. **36**, e1054497. (doi:10.1080/02724634.2015.1054497)
41. Pol D, Rauhut OWM. 2012 A Middle Jurassic abelisaurid from Patagonia and the early diversification of theropod dinosaurs. *Proc. R. Soc. B* **279**, 3170–3175. (doi:10.1098/rspb.2012.0660)
42. Sombathy R, O'Connor PM, D'Emic MD. 2025 Osteohistology of the unusually fast-growing theropod dinosaur *Ceratosaurus*. *J. Anat*. **247**, 765–789. (doi:10.1111/joa.14186)
43. Therrien F, Zelenitsky DK, Tanaka K, Voris JT, Erickson GM, Currie PJ, DeBuhr CL, Kobayashi Y. 2023 Exceptionally preserved stomach contents of a young tyrannosaurid reveal an ontogenetic dietary shift in an iconic extinct predator. *Sci. Adv*. **9**, eadi0505. (doi:10.1126/sciadv.adi0505)
44. Benson RBJ. 2010 A description of *Megalosaurus bucklandii* (Dinosauria: Theropoda) from the Bathonian of the UK and the relationships of Middle Jurassic theropods. *Zool. J. Linn. Soc*. **158**, 882–935. (doi:10.1111/j.1096-3642.2009.00569.x)
45. Hone DWE, Holtz TR. 2017 A century of spinosaurs - a review and revision of the spinosauridae with comments on their ecology. *Acta Geol. Sin.* **91**, 1120–1132. (doi:10.1111/1755-6724.13328)
46. D'Amore DC, Johnson-Ransom E, Snively E, Hone DWE. 2025 Prey size and ecological separation in spinosaurid theropods based on heterodonty and rostrum shape. *Anat. Rec*. **308**, 1331–1348. (doi:10.1002/ar.25563)
47. Foster W, Brusatte SL, Carr TD, Williamson TE, Yi L, Lü J. 2021 The cranial anatomy of the long-snouted tyrannosaurid dinosaur *Qianzhousaurus sinensis* from the Upper Cretaceous of China. *J. Vertebr. Paleontol*. **41**, e1999251. (doi:10.1080/02724634.2021.1999251)
48. Rowe AJ, Rayfield EJ. 2024 Morphological evolution and functional consequences of giantism in tyrannosauroid dinosaurs. *iScience* **27**, 110679. (doi:10.1016/j.isci.2024.110679)
49. Yun CG. 2024 Mandibular force profiles of *Alioramini* (Theropoda: Tyrannosauridae) with implications for palaeoecology of this unique lineage of tyrannosaurid dinosaurs. *Lethaia* **57**, 1–12. (doi:10.18261/let.57.2.6)
50. Rowe AJ, Rayfield EJ. 2025 Carnivorous dinosaur lineages adopt different skull performances at gigantic size. *Curr. Biol*. **35**, 3664–3673. (doi:10.1016/j.cub.2025.06.051)
51. Loewen MA, Irmis RB, Sertich JJW, Currie PJ, Sampson SD. 2013 Tyrant dinosaur evolution tracks the rise and fall of Late Cretaceous oceans. *PLoS One* **8**, e79420. (doi:10.1371/journal.pone.0079420)
52. Brusatte SL, Carr TD. 2016 The phylogeny and evolutionary history of tyrannosauroid dinosaurs. *Sci. Rep*. **6**, 20252. (doi:10.1038/srep20252)
53. Carr TD, Varricchio DJ, Sedlmayr JC, Roberts EM, Moore JR. 2017 A new tyrannosaur with evidence for anagenesis and crocodile-like facial sensory system. *Sci. Rep*. **7**, 44942. (doi:10.1038/srep44942)
54. Voris JT, Zelenitsky DK, Kobayashi Y, Modesto SP, Therrien F, Tsutsumi H, Chinzorig T, Tsogbaatar K. 2025 A new Mongolian tyrannosauroid and the evolution of Eutyrannosauria. *Nature* **642**, 973–979. (doi:10.1038/s41586-025-08964-6)
55. Meso JG, Pol D, Chiappe L, Qin Z, Díaz-Martínez I, Gianechini F, Apesteguía S, Makovicky PJ, Pittman M. 2025 Body size and evolutionary rate analyses reveal complex evolutionary history of Alvarezsauria. *Cladistics* **41**, 135–155. (doi:10.1111/cla.12600)
56. Qin Z, Zhao Q, Choiniere JN, Clark JM, Benton MJ, Xu X. 2021 Growth and miniaturization among alvarezsauroid dinosaurs. *Curr. Biol*. **31**, 3687–3693. (doi:10.1016/j.cub.2021.06.013)
57. Senter PJ. 2023 Restudy of shoulder motion in the theropod dinosaur *Mononykus olecranus* (Alvarezsauridae). *PeerJ* **5**, e16605. (doi:10.7717/peerj.16605)
58. McCurry MR, Fitzgerald EMG, Evans AR, Adams JW, McHenry CR. 2017 Skull shape reflects prey size niche in toothed whales. *Biol. J. Linn. Soc*. **121**, 936–946. (doi:10.1093/biolinnean/blx032)
59. Herrel A, Schaerlaeken V, Meyers JJ, Metzger KA, Ross CF. 2007 The evolution of cranial design and performance in squamates: consequences of skull-bone reduction on feeding behavior. *Integr. Comp. Biol*. **47**, 107–117. (doi:10.1093/icb/icm014)
60. Young MT *et al*. 2012 The cranial osteology and feeding ecology of the metriorhynchid crocodylomorph genera *Dakosaurus* and *Plesiosuchus* from the late Jurassic of Europe. *PLoS One* **7**, e44985. (doi:10.1371/journal.pone.0044985)
61. Hennekam JJ. 2022 Comparative morphology of the dormouse skull and the influence of size and ecology. *J. Anat*. **240**, 914–935. (doi:10.1111/joa.13596)
62. Cost IN, Middleton KM, Sellers KC, Echols MS, Witmer LM, Davis JL, Holliday CM. 2020 Palatal biomechanics and its significance for cranial kinesis in *Tyrannosaurus rex*. *Anat. Rec*. **303**, 999–1017. (doi:10.1002/ar.24219)
63. Johnson-Ransom E, Li F, Xu X, Ramos R, Midzuk AJ, Thon U, Atkins-Weltman K, Snively E. 2024 Comparative cranial biomechanics reveal that Late Cretaceous tyrannosaurids exerted relatively greater bite force than in early-diverging tyrannosauroids. *Anat. Rec*. **307**, 1897–1917. (doi:10.1002/ar.25326)
64. Costa GC, Vitt LJ, Pianka ER, Mesquita DO, Colli GR. 2008 Optimal foraging constrains macroecological patterns: body size and dietary niche breadth in lizards. *Glob. Ecol. Biogeogr.* **17**, 670–677. (doi:10.1111/j.1466-8238.2008.00405.x)
65. Tucker MA, Rogers TL. 2014 Examining the prey mass of terrestrial and aquatic carnivorous mammals: minimum, maximum and range. *PLoS One* **9**, e106402. (doi:10.1371/journal.pone.0106402)
66. Sander PM *et al*. 2011 Biology of the sauropod dinosaurs: the evolution of gigantism. *Biol. Rev*. **86**, 117–155. (doi:10.1111/j.1469-185x.2010.00137.x)
67. Słowiak J, Szczygielski T, Ginter M, Fostowicz-Frelik Ł. 2020 Uninterrupted growth in a non-polar hadrosaur explains the gigantism among duck-billed dinosaurs. *Palaeontology* **63**, 579–599. (doi:10.1111/pala.12473)
68. Fastovsky DE, Smith JB. 2004 Dinosaur paleoecology. In *The Dinosauria* (eds DB Weishampel, H Osmólska, P Dobson), pp. 614–626, 2nd edn. Berkeley, CA: University of California. (doi:10.1525/california/9780520242098.003.0029)
69. Carpenter K, Sanders F, McWhinney LA, Wood L. 2005 Evidence for predator-prey relationships: examples for *Allosaurus* and *Stegosaurus*. In *The carnivorous dinosaurs* (ed. K Carpenter), pp. 325–350. Bloomington and Indianapolis, IN: Indiana University Press.
70. Motta MJ, Aranciaga Rolando AM, Rozadilla S, Agnolin FE, Chimento NR, Egli FB, Novas FE. 2016 New theropod fauna from the Upper Cretaceous (Huincul Formation) of northwestern Patagonia, Argentina. *N. M. Mus. Nat. Hist. Bull*. **71**, 231–253.
71. Coria RA, Currie PJ. 2006 A new carcharodontosaurid (Dinosauria, Theropoda) from the Upper Cretaceous of Argentina. *Geodiversitas* **28**, 71–118.

72. Therrien F, Henderson DM, Ruff CB. 2005 Bite me: biomechanical models of theropod mandibles and implications for feeding. In *The carnivorous dinosaurs. life of the past* (ed. K Carpenter), pp. 179–237. Bloomington, IN: Indiana University Press.
73. Erickson GM, Olson KH. 1996 Bite marks attributable to *Tyrannosaurus rex*: preliminary description and implications. *J. Vertebr. Paleontol*. **16**, 175–178. (doi:10.1080/02724634.1996.10011297)
74. Rivera Sylva HE, Hone DW, Dodson P. 2012 Bite marks of a large theropod on an hadrosaur limb bone from Coahuila, Mexico. *Bol. De La Soc. Geológica Mex* **64**, 157–161. (doi:10.18268/BSGM2012v64n1a11)
75. Fowler DW, Sullivan RM. 2016 A ceratopsid pelvis with toothmarks from the Upper Cretaceous Kirtland Formation, New Mexico: evidence of late Campanian tyrannosaurids feeding behaviour. *N. M. Mus. Nat. Hist. Sci. Bull*. **35**, 127–130.
76. DeLong JP, Hanley TC, Vasseur DA. 2014 Predator–prey dynamics and the plasticity of predator body size. *Funct. Ecol*. **28**, 487–493. (doi:10.1111/1365-2435.12199)
77. Brown CM, Henderson DM, Vinther J, Fletcher I, Sistiaga A, Herrera J, Summons RE. 2017 An exceptionally preserved three-dimensional armored dinosaur reveals insights into coloration and cretaceous predator-prey dynamics. *Curr. Biol.* **27**, 2514–2521. (doi:10.1016/j.cub.2017.06.071)
78. Cohen J. 1988 *Statistical power analysis for the behavioural sciences*, 2nd edn. New York, NY: Lawrence Erlbaum Associates.
79. Wainwright PC, Alfaro ME, Bolnick DI, Hulsey CD. 2005 Many-to-one mapping of form to function: a general principle in organismal design? *Integr. Comp. Biol*. **45**, 256–262. (doi:10.1093/icb/45.2.256)
80. Dececchi TA, Larsson HCE. 2013 Body and limb size dissociation at the origin of birds: uncoupling allometric constraints across a macroevolutionary transition. *Evolution* **67**, 2741–2752. (doi:10.1111/evo.12150)
81. Chin DD, Matloff LY, Stowers AK, Tucci ER, Lentink D. 2017 Inspiration for wing design: how forelimb specialization enables active flight in modern vertebrates. *J. R. Soc. Interface* **14**, 20170240. (doi:10.1098/rsif.2017.0240)
82. Yun CG. 2024 Evaluating the paleoecology of the Megaraptora (Dinosauria: Theropoda) through biomechanical approaches Evaluación de la paleoecología de Megaraptora (Dinosauria: Theropoda) mediante enfoques biomecánicos. *Span. J. Palaeontol.* **39**, 223–234. (doi:10.7203/sjp.29797)
83. Supplementary information for: Drivers and mechanisms of convergent forelimb reduction in non-avian theropod dinosaurs. Figshare. (doi:10.6084/m9.figshare.30374509)